

# Type-1.5 superconductivity in multiband systems: magnetic response, broken symmetries and microscopic theory. A brief overview.

E. Babaev<sup>1,2</sup>, J. Carlström<sup>1,2</sup>, J. Garaud<sup>2</sup>, M. Silaev<sup>1,3</sup> and J.M. Speight<sup>4</sup>

<sup>1</sup> *Department of Theoretical Physics, The Royal Institute of Technology, Stockholm, SE-10691 Sweden*

<sup>2</sup> *Department of Physics, University of Massachusetts Amherst, MA 01003 USA*

<sup>3</sup> *Institute for Physics of Microstructures RAS, 603950 Nizhny Novgorod, Russia.*

<sup>4</sup> *School of Mathematics, University of Leeds, Leeds LS2 9JT, UK*

A conventional superconductor is described by a single complex order parameter field which has two fundamental length scales, the magnetic field penetration depth  $\lambda$  and the coherence length  $\xi$ . Their ratio  $\kappa$  determines the response of a superconductor to an external field, sorting them into two categories as follows; type-I when  $\kappa < 1/\sqrt{2}$  and type-II when  $\kappa > 1/\sqrt{2}$ . We overview here multicomponent systems which can possess three or more fundamental length scales and allow a separate “type-1.5” superconducting state when, e.g. in two-component case  $\xi_1 < \sqrt{2}\lambda < \xi_2$ . In that state, as a consequence of the extra fundamental length scale, vortices attract one another at long range but repel at shorter ranges. As a consequence the system should form an additional Semi-Meissner state which properties we discuss below. In that state vortices form clusters in low magnetic fields. Inside the cluster one of the component is depleted and the superconductor-to-normal interface has negative energy. In contrast the current in second component is mostly concentrated on the cluster’s boundary, making the energy of this interface positive. Here we briefly overview recent developments in Ginzburg-Landau and microscopic descriptions of this state. Prepared for the proceedings of Vortex VII conference, Rhodes September 2011.

## I. INTRODUCTION

Type-I superconductors expel weak magnetic fields, while strong fields give rise to formation of macroscopic normal domains with magnetic flux.<sup>1-3</sup> The response of type-II superconductors is different;<sup>4</sup> below some critical value  $H_{c1}$ , the field is expelled. Above this value a superconductor forms a lattice or a liquid of vortices which carry magnetic flux through the system. Only at a higher second critical value,  $H_{c2}$  superconductivity is destroyed.

These different responses are usually viewed as consequences of the vortex interaction in these systems, the energy cost of a boundary between superconducting and normal states and the thermodynamic stability of vortex excitations. In a type-II superconductor the energy cost of a boundary between the normal and the superconducting state is negative, while the interaction between vortices is repulsive.<sup>4</sup> This leads to a formation of stable vortex lattices and liquids. In type-I superconductors the situation is the opposite; the vortex interaction is attractive (thus making them unstable against collapse into one large “giant” vortex), while the boundary energy between normal and superconducting states is positive.

One can distinguish also a special “zero measure” boundary case where  $\kappa$  has a critical value exactly at the type-I/type-II boundary, which in the most common GL model parameterization corresponds to  $\kappa = 1/\sqrt{2}$ . In that case vortices do not interact<sup>5,6</sup> in the Ginzburg-Landau theory. The noninteracting regime, which is frequently called “Bogomolny limit” is a property of Ginzburg-Landau model where, at  $\kappa = 1/\sqrt{2}$ , the core-core attractive interaction between vortices exactly cancels the current-current repulsive interaction.<sup>5,6</sup> However indeed in a realistic system even in the limit  $\kappa = 1/\sqrt{2}$ , there will be always leftover inter-vortex interactions, appearing beyond the GL field theoretic description, from underlying microscopic physics. The form of that interaction potential is determined not by the fundamental length scales of the GL theory but by non-universal microscopic physics and it can indeed be non-monotonic.<sup>7</sup> These microscopic corrections are extremely small, however they can be relevant not only at  $\kappa = 1/\sqrt{2}$  but also in a very narrow window of parameters near  $\kappa \approx 1/\sqrt{2}$  where intervortex forces in GL theory are also very small. We do not consider the physics which arises in the Bogomolny limits in this paper, rather concentrating on the physics associated with fundamental modes of GL field theory.

Recently there has been increased interest in superconductors with several superconducting components. The Ginzburg-Landau free energy functional for multicomponent system has the form

$$F = \frac{1}{2} \sum_i (D\psi_i)(D\psi_i)^* + V(|\psi_i|) + \frac{1}{2}(\nabla \times \mathbf{A})^2 \quad (1)$$

Here  $\psi_i$  are complex superconducting components,  $D = \nabla + ie\mathbf{A}$ , and  $\psi_a = |\psi_a|e^{i\theta_a}$ ,  $a = 1, 2$ , and  $V(|\psi_i|)$  stands for effective potential. Depending on symmetry of the system there can also be present mixed (with respect to components  $\psi_i$ ) gradient terms (for a more detailed review see<sup>8</sup>).

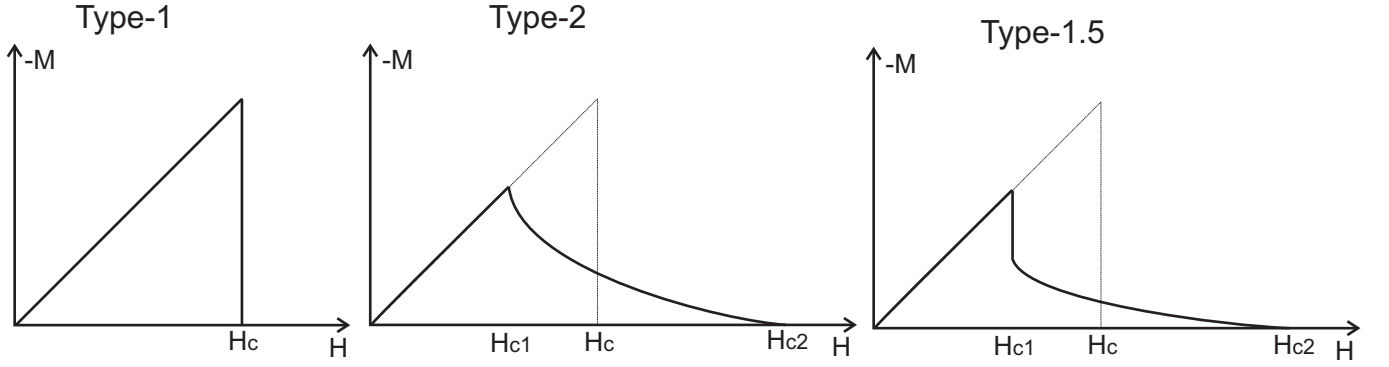


FIG. 1. A schematic picture of magnetization curves of type-I, type-II and type-1.5 superconductors.

The main situations where multiple superconducting components arise are (i) multiband superconductors<sup>9-18</sup> (where  $\psi_i$  represent condensates belonging to different bands), (ii) mixtures of independently conserved condensates such as the projected superconductivity in metallic hydrogen and hydrogen rich alloys,<sup>19-23</sup> (where  $\psi_i$  represent electronic and protonic Cooper pairs or deuteronic condensate) or models of nuclear superconductors in neutron stars interior<sup>24</sup> (where  $\psi_i$  represent protonic and  $\Sigma^-$  hyperonic condensates) and (iii) superconductors with other than s-wave pairing symmetries. The principal difference between the cases (i) and (ii) is the absence of the intercomponent Josephson coupling in case of system like metallic hydrogen (ii) because there the condensates are independently conserved. Thus the symmetry is  $U(1) \times U(1)$  or higher. In the case (i) multiple superconducting components originate from Cooper pairing in different bands. Because condensates in different bands are not independently conserved there is a rather generic presence of intercomponent Josephson coupling  $\frac{\eta}{2}(\psi_1\psi_2^* + \psi_2\psi_1^*)$  in that case.

### A. Type-1.5 superconductivity

The possibility of a new type of superconductivity, distinct from the type-I and type-II in multicomponent systems<sup>8,25-29</sup> comes from the following considerations. In principle the boundary problem in the Ginzburg-Landau type of equations in the presence of phase winding is *not* reducible to a one-dimensional problem in general. Furthermore, as discussed in,<sup>8,25,26,28-30</sup> in general in two-component models there are three fundamental length scales: magnetic field penetration length  $\lambda$  and two characteristic length scales of the variations of the density fields  $\xi_1, \xi_2$  which renders the model impossible to parametrize in terms of a single dimensionless parameter  $\kappa$  and thus the type-I/type-II dichotomy is not sufficient for classification. Rather, in a wide range of parameters, as a consequence of the existence of three fundamental length scales, there is a separate superconducting regime with  $\xi_1/\sqrt{2} < \lambda < \xi_2/\sqrt{2}$ . In that regime a situation is possible where vortices have long-range attractive (due to “outer cores” overlap), short-range repulsive interaction (driven by current-current and electromagnetic interaction) and form vortex clusters immersed in domains of two-component Meissner state.<sup>25,26</sup> Recent experimental works<sup>27,31</sup> proposed that this state is realized in the two-band material  $\text{MgB}_2$ . In Ref.<sup>27</sup> this regime was termed “type-1.5” superconductivity by Moshchalkov et al. These works resulted in increasing interest in the subject.<sup>32-35</sup> Recently type-1.5 superconductivity was discussed in context of quantum Hall effect.<sup>36</sup>

If the vortices form clusters one cannot use the usual one-dimensional argument concerning the energy of superconductor-to-normal state boundary to classify the magnetic response of the system. First of all, the energy per vortex in such a case depends on whether a vortex is placed in a cluster or not. Formation of a single isolated vortex might be energetically unfavorable, while formation of vortex clusters is favorable, because in a cluster where vortices are placed in a minimum of the interaction potential, the energy per flux quantum is smaller than that for an isolated vortex.

Thus, besides the energy of a vortex in a cluster, there appears an additional energy characteristic associated with the boundary of a cluster.

We summarize the basic properties of type-I, type-II and type-1.5 regimes in the table I.<sup>8</sup>

	single-component Type-I	single-component Type-II	multi-component Type-1.5
<b>Characteristic lengths scales</b>	Penetration length $\lambda$ & coherence length $\xi$ ( $\frac{\lambda}{\xi} < \frac{1}{\sqrt{2}}$ )	Penetration length $\lambda$ & coherence length $\xi$ ( $\frac{\lambda}{\xi} > \frac{1}{\sqrt{2}}$ )	Two characteristic density variations length scales $\xi_1, \xi_2$ and penetration length $\lambda$ , the non-monotonic vortex interaction occurs in these systems in a large range of parameters when $\xi_1 < \sqrt{2}\lambda < \xi_2$
<b>Intervortex interaction</b>	Attractive	Repulsive	Attractive at long range and repulsive at short range
<b>Energy of superconducting/normal state boundary</b>	Positive	Negative	Under quite general conditions negative energy of superconductor/normal interface inside a vortex cluster but positive energy of the vortex cluster's boundary
<b>The magnetic field required to form a vortex</b>	Larger than the thermodynamical critical magnetic field	Smaller than thermodynamical critical magnetic field	In different cases either (i) smaller than the thermodynamical critical magnetic field or (ii) larger than critical magnetic field for single vortex but smaller than critical magnetic field for a vortex cluster of a certain critical size
<b>Phases in external magnetic field</b>	(i) Meissner state at low fields; (ii) Macroscopically large normal domains at larger fields. First order phase transition between superconducting (Meissner) and normal states	(i) Meissner state at low fields, (ii) vortex lattices/liquids at larger fields. Second order phase transitions between Meissner and vortex states and between vortex and normal states at the level of mean-field theory.	(i) Meissner state at low fields (ii) "Semi-Meissner state": vortex clusters coexisting with Meissner domains at intermediate fields (iii) Vortex lattices/liquids at larger fields. Vortices form via a first order phase transition. The transition from vortex states to normal state is second order.
<b>Energy <math>E(N)</math> of N-quantum axially symmetric vortex solutions</b>	$\frac{E(N)}{N} < \frac{E(N-1)}{N-1}$ for all N. Vortices collapse onto a single N-quantum mega-vortex	$\frac{E(N)}{N} > \frac{E(N-1)}{N-1}$ for all N. N-quantum vortex decays into N infinitely separated single-quantum vortices	There is a characteristic number $N_c$ such that $\frac{E(N)}{N} < \frac{E(N-1)}{N-1}$ for $N < N_c$ , while $\frac{E(N)}{N} > \frac{E(N-1)}{N-1}$ for $N > N_c$ . N-quantum vortices decay into vortex clusters.

TABLE I. Basic characteristics of bulk clean superconductors in type-I, type-II and type-1.5 regimes. Here the most common units are used in which the value of the GL parameter which separates type-I and type-II regimes in a single-component theory is  $\kappa_c = 1/\sqrt{2}$ . Magnetization curves in these regimes are shown on Fig. 1

## B. Generalization to N-component case.

The concept of type-1.5 superconductivity has a straightforward generalization to N-component case. There it can occur in systems where characteristic length scales are  $\xi_1, \dots, \xi_k < \sqrt{2}\lambda < \xi_{k+1}, \dots, \xi_N$  and there are thermodynamically stable vortices with non-monotonic interaction.

## II. THE TWO-BAND GINZBURG-LANDAU MODEL WITH ARBITRARY INTERBAND INTERACTIONS. DEFINITION OF THE LENGTH SCALES AND TYPE-1.5 REGIME

### A. Free energy functional

In this section we study the type-1.5 regime using the following two-component Ginzburg-Landau (TCGL) free energy functional.

$$F = \frac{1}{2}(D\psi_1)(D\psi_1)^* + \frac{1}{2}(D\psi_2)(D\psi_2)^* - \nu Re\left\{(D\psi_1)(D\psi_2)^*\right\} + \frac{1}{2}(\nabla \times \mathbf{A})^2 + F_p \quad (2)$$

Here  $D = \nabla + ie\mathbf{A}$ , and  $\psi_a = |\psi_a|e^{i\theta_a}$ ,  $a = 1, 2$ , represent two superconducting components which, in a two-band superconductor are associated with two different bands. The term  $F_p$  can contain in our analysis an *arbitrary* collection of non-gradient terms representing various inter and intra-band interactions. Below we show how three characteristic length scales are defined in this two component model (two associated with densities variations and the London magnetic field penetration length). Note that existence of two bands in a superconductor is *not* a sufficient conditions for a superconductor to be described by a model like (2) with two well-defined coherence lengths. Conditions of appearance of regimes when the system does not allow a description in terms of two-component fields theory (2) is discussed in the work based on microscopic considerations.<sup>28,29</sup> This kind of two-band GL models were also derived earlier from microscopic two-band theories at elevated temperature close, but not too close to  $T_c$ .<sup>12-14</sup> Although some other recent works proposed to keep higher order gradient terms in GL expansion,<sup>37</sup> however in Ref.<sup>29</sup> it was demonstrated that the minimal two-band model (2) is microscopically justified on formal grounds and gives a very good description of the system in a wide range of temperatures.

The only vortex solutions of the model (2) which have finite energy per unit length are the integer  $N$ -flux quantum vortices which have the following phase windings along a contour  $l$  around the vortex core:  $\oint_l \nabla\theta_1 = 2\pi N$ ,  $\oint_l \nabla\theta_2 = 2\pi N$  which can be denoted as (N,N). Vortices with differing phase windings (N,M) carry a fractional multiple of the magnetic flux quantum and have energy divergent with the system size.<sup>43</sup>

In what follows we investigate only the integer flux vortex solutions which are the energetically cheapest objects to produce by means of an external field in a bulk superconductor. Note that since this object is essentially a bound state of two vortices, it in general will have two different co-centered cores.

### III. INTERVORTEX FORCES AT LONG RANGE

In this section we explain how the nature (attractive or repulsive) of the forces between well separated vortices in system (2) can be determined purely by analyzing  $F_p$  and how three fundamental length scales can be defined in the model (2). Below we will analyze system (2) in the case  $\nu = 0$  but for an arbitrary effective potential. Detailed discussion of the effects of mixed gradient terms can be found in<sup>8</sup> By gauge invariance,  $F_p$  may depend only on  $|\psi_1|$ ,  $|\psi_2|$  and  $\delta = \theta_1 - \theta_2$ . We consider the regime that it has a global minimum at some point other than the one with  $|\psi_a| = 0$ . We may assume, without loss of generality, that the minimum of  $F$  is at  $(|\psi_1|, |\psi_2|, \delta) = (u_1, u_2, 0)$  where  $u_1 > 0$  and  $u_2 \geq 0$ . Then the model has a trivial solution,  $\psi_1 = u_1$ ,  $\psi_2 = u_2$ ,  $A = 0$ , which we call the ground state. It also supports vortex solutions of the form

$$\psi_a = f_a(r)e^{i\theta}, \quad (A_1, A_2) = \frac{a(r)}{r}(-\sin\theta, \cos\theta) \quad (3)$$

where  $f_1, f_2, a$  are real profile functions with boundary behavior  $f_a(0) = a(0) = 0$ ,  $f_a(\infty) = u_a$ ,  $a(\infty) = -1/e$ . No explicit expressions for  $f_a, a$  are known, but, by analyzing the system of differential equations they satisfy, one can construct asymptotic expansions for them at large  $r$ , see.<sup>8,26</sup>

At large  $r$  from the vortex in the model (2) the system recovers (up to exponentially small corrections) the ground state. In fact, the long-range field behavior of a vortex solution can be identified with a solution of the *linearization* of the model about the ground state, in the presence of appropriate point sources at the vortex core. This idea is explained in detail for single component GL theory in.<sup>38</sup> A common feature of topological solitons (vortices being a particular example) is that the forces they exert on one another coincide asymptotically (at large separation) with those between the corresponding point sources interacting via the linearized field theory.<sup>39</sup> For (2), the linearization has one vector ( $A$ ) and 3 real scalar ( $\epsilon_1 = |\psi_1| - u_1$ ,  $\epsilon_2 = |\psi_2| - u_2$  and  $\delta$ ) degrees of freedom. The isolated vortex solutions have, by definition within the ansatz we use,  $\delta \equiv 0$  everywhere. Note that the GL system may also possess non-axially-symmetric solutions, such as vortex clusters, and for these there is no reason why  $\delta$  should vanish everywhere and in fact it does not.<sup>30</sup> However below we first consider a single vortex using a axially-symmetric ansatz, and hence have no source for  $\delta$ , so we can set  $\delta = 0$  in the linearization, which becomes

$$F_{lin} = \frac{1}{2}|\nabla\epsilon_1|^2 + \frac{1}{2}|\nabla\epsilon_2|^2 + \frac{1}{2}\begin{pmatrix} \epsilon_1 \\ \epsilon_2 \end{pmatrix} \cdot \mathcal{H} \begin{pmatrix} \epsilon_1 \\ \epsilon_2 \end{pmatrix} + \frac{1}{2}(\partial_1 A_2 - \partial_2 A_1)^2 + \frac{1}{2}e^2(u_1^2 + u_2^2)|A|^2. \quad (4)$$

Here,  $\mathcal{H}$  is the Hessian matrix of  $F_p(|\psi_1|, |\psi_2|, 0)$  about  $(u_1, u_2)$ , that is,

$$\mathcal{H}_{ab} = \left. \frac{\partial^2 F_p}{\partial |\psi_a| \partial |\psi_b|} \right|_{(u_1, u_2, 0)}. \quad (5)$$

Note that, in  $F_{lin}$ , the vector field  $A$  decouples from the scalar fields and mediates a repulsive force between vortices (originating in current-current and magnetic interaction) with decay length which is the penetration length  $\lambda = 1/\mu_A$  where  $\mu_A$  is the mass of the field, that is,

$$\mu_A = e\sqrt{u_1^2 + u_2^2}. \quad (6)$$

By contrast, the scalar fields  $\epsilon_1, \epsilon_2$  are, in general, coupled (i.e. in general the symmetric matrix  $\mathcal{H}$  has off-diagonal terms). To remove these we make a linear redefinition of fields, expanding  $(\epsilon_1, \epsilon_2)^T$  with respect to the orthonormal basis for  $\mathbb{R}^2$  formed by the eigenvectors  $v_1, v_2$  of  $\mathcal{H}$ ,

$$(\epsilon_1, \epsilon_2)^T = \chi_1 v_1 + \chi_2 v_2. \quad (7)$$

The corresponding eigenvalues  $\mu_1^2, \mu_2^2$  are necessarily real (since  $\mathcal{H}$  is symmetric) and positive (since  $(u_1, u_2)$  is a minimum of  $F_p$ ), and hence

$$F_{lin} = \frac{1}{2} \sum_{a=1}^2 (|\nabla \chi_a|^2 + \mu_a^2 \chi_a^2) + \frac{1}{2} (\partial_1 A_2 - \partial_2 A_1)^2 + \frac{1}{2} e(u_1^2 + u_2^2) |A|^2. \quad (8)$$

The scalar fields  $\chi_1, \chi_2$  each mediate an attractive force between vortices, with length scales

$$\xi_1 \equiv 1/\mu_1, \quad \xi_2 \equiv 1/\mu_2 \quad (9)$$

respectively. Physically these interactions are associated with the attractive core-core interactions. We can be somewhat more quantitative. In terms of the normal-mode fields  $\chi_1, \chi_2$  and  $A$ , the composite point source which must be introduced into  $F_{lin}$  to produce field configurations identical to those of vortex asymptotics is

$$\kappa_1 = q_1 \delta(x), \quad \kappa_2 = q_2 \delta(x), \quad \mathbf{j} = m(\partial_2, -\partial_1) \delta(x), \quad (10)$$

where  $\kappa_1$  is the source for  $\chi_1$ ,  $\kappa_2$  the source for  $\chi_2$ ,  $\mathbf{j}$  the source for  $\mathbf{A}$ ,  $\delta(x)$  denotes the two dimensional Dirac delta distribution and  $q_1, q_2$  and  $m$  are unknown real constants which can, in principle, be determined numerically by a careful analysis of the vortex asymptotics. Physically, a vortex, as seen from a long distance can be thought of as a point particle carrying two different types of scalar monopole charge,  $q_1, q_2$ , inducing fields of mass  $\mu_1, \mu_2$  respectively, and a magnetic dipole moment  $m$  oriented orthogonal to the  $x_1 x_2$  plane, inducing a massive vector field of mass  $\mu_A$ . The interaction energy experienced by a pair of point particles carrying these sources, held distance  $r$  apart, is easily computed in linear field theory. For example, two scalar monopoles of charge  $q$  inducing fields of mass  $\mu$  held at positions  $\mathbf{y}$  and  $\tilde{\mathbf{y}}$  in  $\mathbb{R}^2$  experience interaction energy

$$E_{int} = - \int_{\mathbb{R}^2} \kappa \tilde{\chi} = - \int_{\mathbb{R}^2} q \delta(\mathbf{x} - \mathbf{y}) \frac{q}{2\pi} K_0(\mu|\mathbf{y} - \tilde{\mathbf{y}}|) = - \frac{q^2}{2\pi} K_0(\mu|\mathbf{y} - \tilde{\mathbf{y}}|) \quad (11)$$

where  $\kappa$  is the source for the monopole at  $\mathbf{y}$ ,  $\tilde{\chi}$  is the scalar field induced by the monopole at  $\tilde{\mathbf{y}}$ <sup>38</sup> and  $K_0$  denotes the modified Bessel's function of the second kind. The interaction energy for a pair of magnetic dipoles may be computed similarly. In the case of our two component GL model, the total interaction energy has three terms, corresponding to the three sources in the composite point source (10), and turns out to be

$$E_{int} = \frac{m^2}{2\pi} K_0(\mu_A r) - \frac{q_1^2}{2\pi} K_0(\mu_1 r) - \frac{q_2^2}{2\pi} K_0(\mu_2 r). \quad (12)$$

Note that, the first term in this formula which originates in magnetic and current-current interaction is repulsive, while the other two as associated with core-core interactions of two kinds of cores are attractive. At very large  $r$ ,  $E_{int}(r)$  is dominated by whichever term corresponds to the smallest of the three masses,  $\mu_A, \mu_1, \mu_2$ , so to determine whether vortices attract at long range, it is enough to compute just these masses.

To summarize, the nature of intervortex forces at large separation can be determined purely by analyzing  $F_p$ : one finds the ground state  $(u_1, u_2)$  and the Hessian  $\mathcal{H}$  of  $F_p$  about  $(u_1, u_2)$ . From this one computes the mass of the vector field  $A$ ,  $\mu_A = e\sqrt{u_1^2 + u_2^2}$ , and the masses  $\mu_1, \mu_2$  of the scalar normal modes (the fields  $\chi_1, \chi_2$ ), these masses being the square roots of the eigenvalues of  $\mathcal{H}$ . If either (or both) of  $\mu_1, \mu_2$  are less than  $\mu_A$ , then the dominant interaction at long range is attractive (i.e. vortex core extends beyond the area where magnetic field is localized), while if  $\mu_A$  is less than both  $\mu_1$  and  $\mu_2$ , the dominant interaction at long range is repulsive. The special feature of the two-component model is that the vortices where core extends beyond the magnetic field penetration length are

thermodynamically stable in a range of parameters and moreover one can have a repulsive force between the vortices at shorter distances.<sup>8,25,26</sup> It is important to stress that length scales  $\mu_1^{-1}, \mu_2^{-1}$  are not directly associated with the individual condensates  $\psi_1, \psi_2$ . Rather they are associated with the normal modes  $\chi_1, \chi_2$ , defined as<sup>8,26</sup>

$$\chi_1 = (|\psi_1| - u_1) \cos \Theta - (|\psi_2| - u_2) \sin \Theta, \quad \chi_2 = -(|\psi_1| - u_1) \sin \Theta - (|\psi_2| - u_2) \cos \Theta. \quad (13)$$

These may be thought of as rotated (in field space) versions of  $\epsilon_1 = |\psi_1| - u_1$ ,  $\epsilon_2 = |\psi_2| - u_2$ . The *mixing angle*, that is, the angle between the  $\chi$  and  $\epsilon$  axes, is  $\Theta$ , where the eigenvector  $v_1$  of  $\mathcal{H}$  is  $(\cos \Theta, \sin \Theta)^T$ . This, again, can be determined directly from  $\mathcal{H}$ .

Note also that the shorter of the length scales  $\mu_1^{-1}, \mu_2^{-1}$ , although being a fundamental length scale of the theory, can be masked in a density profile of a vortex solution by nonlinear effects. This, for example certainly happens if  $\mu_1^{-1} \ll \mu_A \equiv \lambda^{-1}$  (see short discussion in Ref.<sup>8</sup>). Also note that in general the minimum of the interaction potential will not be located at the London penetration length, because it in general will be also affected by nonlinearities.

### A. Passive band superconductors

To illustrate the analysis presented above, we consider the simple case of a two band superconductor where one of the bands is passive, that is, with a potential of the form

$$F_p = -\alpha_1 |\psi_1|^2 + \frac{\beta_1}{2} |\psi_1|^2 + \alpha_2 |\psi_2|^2 - \gamma (\psi_1 \bar{\psi}_2 + \bar{\psi}_1 \psi_2) \quad (14)$$

where  $\alpha_j, \beta_1, \gamma$  are positive constants. Then  $F_p$  is minimized when  $\psi_1$  and  $\psi_2$  have equal phase, and have moduli

$$|\psi_1| = u_1 = \sqrt{\frac{\alpha_1}{\beta_1} \left(1 + \frac{\gamma^2}{\alpha_1 \alpha_2}\right)}, \quad |\psi_2| = u_2 = \frac{\gamma}{\alpha_2} u_1. \quad (15)$$

The mass of the vector field  $A$  is

$$\mu_A = e \sqrt{u_1^2 + u_2^2} = e u_1 \sqrt{1 + \frac{\gamma^2}{\alpha_2^2}}. \quad (16)$$

The Hessian matrix of  $F_p$  about  $(u_1, u_2)$  is

$$\mathcal{H} = \begin{pmatrix} 4\alpha_1 + \frac{6\gamma^2}{\alpha_2} & -2\gamma \\ -2\gamma & 2\alpha_2 \end{pmatrix}. \quad (17)$$

It is straightforward to compute explicit expressions for the eigenvalues  $\mu_1^2, \mu_2^2$  of this matrix. These are somewhat complicated, but power series expansion in  $\gamma$  reveals that

$$\mu_1 = 2\sqrt{\alpha_1} + O(\gamma^2), \quad \mu_2 = \sqrt{2\alpha_2} + O(\gamma^2). \quad (18)$$

Similarly, the normalized eigenvector associated with eigenvalue  $\mu_1^2$  is

$$v_1 = \begin{pmatrix} 1 \\ -(2\alpha_1 - \alpha_2)^{-1} \gamma \end{pmatrix} + O(\gamma^2) \quad (19)$$

so the normal modes of fluctuation about the ground state are rotated through a mixing angle

$$\Theta = -(2\alpha_1 - \alpha_2)^{-1} \gamma + O(\gamma^2). \quad (20)$$

In comparison with the uncoupled model ( $\gamma = 0$ ) then, we see that, for small coupling  $\gamma$  the length scales  $1/\mu_A, 1/\mu_1, 1/\mu_2$  are unchanged to leading order, but the normal modes with which  $1/\mu_1, 1/\mu_2$  are associated are mixed to leading order. In particular, there are large regions of parameter space where  $\mu_2 < \mu_A < \mu_1$ , so that vortices attract at long range, even though the active band,  $\psi_1$ , is naively “type II” (that is,  $\beta_1 > e^2/4$ ).



#### IV. VORTEX CLUSTERS IN A SEMI-MEISSNER STATE AND NON-PAIRWISE INTERVORTEX FORCES.

##### A. Model

In this section, following Ref.<sup>30</sup> we consider in more detail two-component Ginzburg-Landau models, with and without Josephson coupling  $\eta$  which directly couples the two condensates (for treatment of other kinds of interband couplings see<sup>8</sup>). When  $\eta = 0$  the condensates are coupled electromagnetically.

$$\mathcal{F} = \frac{1}{2} \sum_{i=1,2} \left[ |(\nabla + ie\mathbf{A})\psi_i|^2 + (2\alpha_i + \beta_i|\psi_i|^2)|\psi_i|^2 \right] + \frac{1}{2}(\nabla \times \mathbf{A})^2 - \eta|\psi_1||\psi_2|\cos(\theta_2 - \theta_1) \quad (21)$$

Here again, the gauge covariant derivative is  $D = \nabla + ie\mathbf{A}$ , and  $\psi_i = |\psi_i|e^{i\varphi_i}$  are complex fields representing the superconducting components. As will be discussed in Sec. VI, calculations based on microscopic two-band Eilenberger theory show that the model (21) can be used to study vortex physics in multiband superconductor for a wide range of parameters.

We also discuss importance of complicated non-pairwise forces between superconducting vortices arising in certain cases in multicomponent systems.<sup>30,40</sup> These non-pairwise forces in certain cases have important consequences for vortex clusters formation in the type-1.5 regime.

##### B. Vortex clusters in a Semi-Meissner state and non-pairwise interactions.

In this section we allow fluctuations in phase difference. When there is non-zero interband Josephson coupling. The phase difference is associated with a massive mode. Its mass is  $\sqrt{\eta(u_1^2 + u_2^2)}/u_1u_2$ .

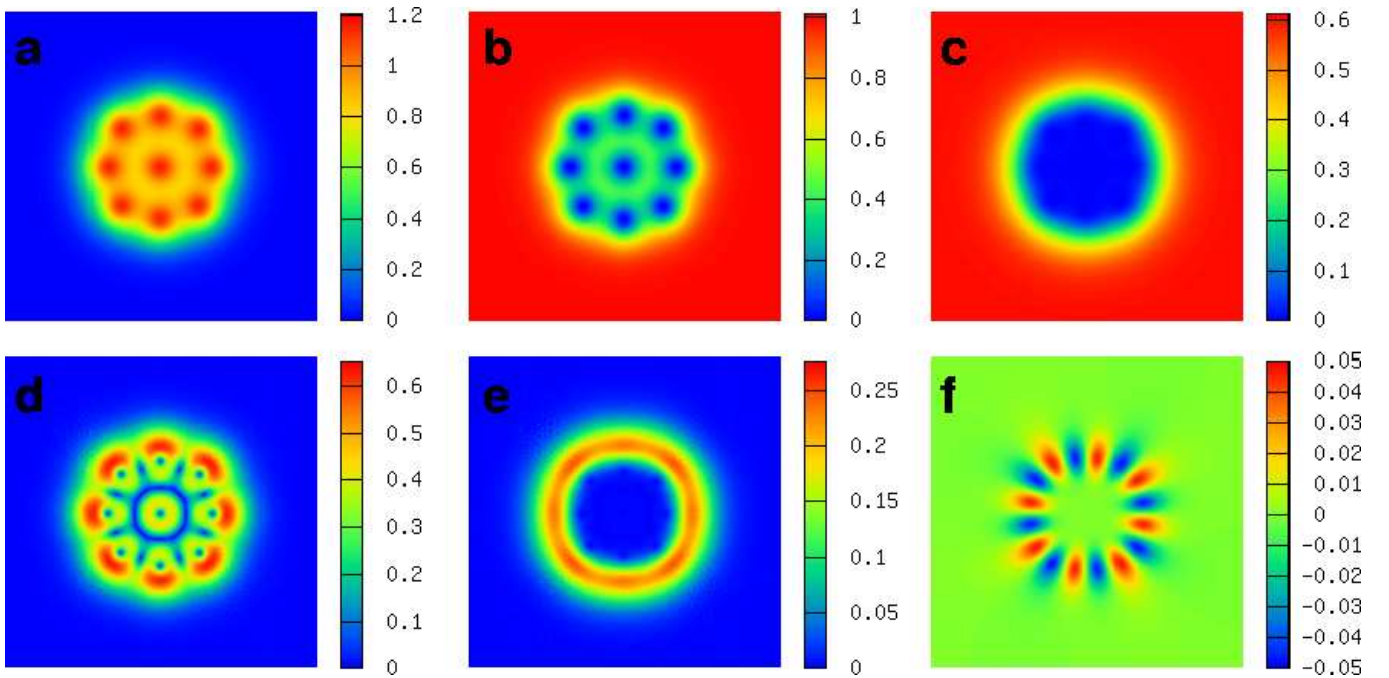


FIG. 2. Ground state of  $N_v = 9$  flux quanta in a type-1.5 superconductor enjoying  $U(1) \times U(1)$  symmetry of the potential (*i.e.*  $\eta = 0$ ). The parameters of the potential being here  $(\alpha_1, \beta_1) = (-1.00, 1.00)$  and  $(\alpha_2, \beta_2) = (-0.60, 1.00)$ , while the electric charge is  $e = 1.48$ . The displayed physical quantities are **a** the magnetic flux density, **b** (*resp.* **c**) is the density of the first (*resp.* second) condensate  $|\psi_{1,2}|^2$ . **d** (*resp.* **e**) shows the norm of the supercurrent in the first (*resp.* second) component. Panel **f** is  $\text{Im}(\psi_1^* \psi_2) \equiv |\psi_1||\psi_2|\sin(\theta_2 - \theta_1)$  being nonzero when there appears a difference between the two condensates. Parameters are chosen so that the second component has a type-I like behavior while the first one tends to form well separated vortices. The density of the second band is depleted in the vortex cluster and its current is mostly concentrated on the boundary of the cluster (see Ref.<sup>30</sup>).

Fig. 2 and Fig. 3 show numerical solutions for N-vortex bound states in several regimes (for technical details see Appendix of<sup>30</sup>). A Nonlinear Conjugate Gradient scheme was used to solve the finite element formulation of the variational problem, within the framework provided by the Freefem++ library.<sup>41</sup> Animations showing the evolution of the system, during the numerical energy minimization, from the various initial configurations to the vortex clusters in the energy minimization process can be found online.<sup>42</sup> The common aspect of the regimes shown on these figures is that the density of one of the components is depleted in the vortex cluster and has its current most concentrated on the boundary of the vortex cluster (i.e. has a type-I like behavior). At the same time the second component forms a full-fledged vortex lattice inside the vortex cluster (i.e. has a type-II-like behavior).

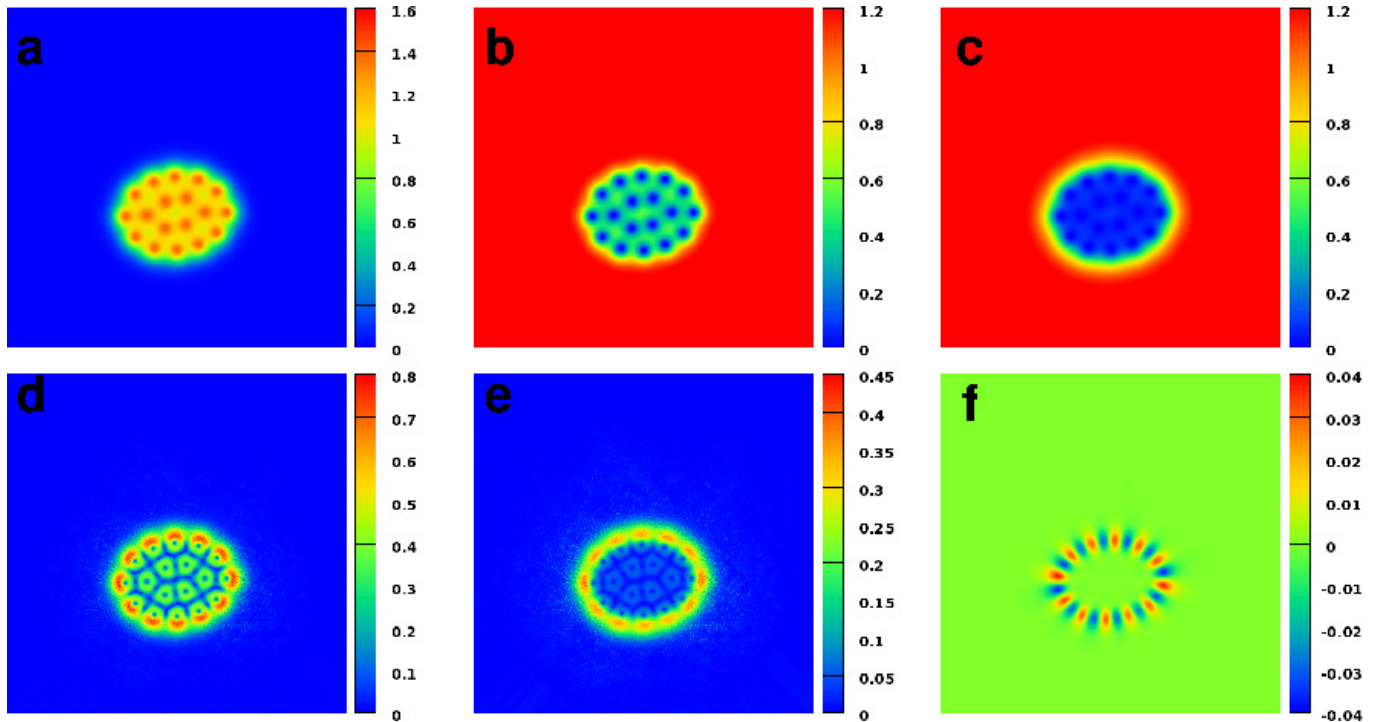


FIG. 3. Elongated ground state cluster of 18 vortices in a superconductor with two active bands. Parameters of the interacting potential are  $(\alpha_1, \beta_1) = (-1.00, 1.00)$ ,  $(\alpha_2, \beta_2) = (-0.0625, 0.25)$  while the interband coupling is  $\eta = 0.5$ . The electric charge, parameterizing the penetration depth of the magnetic field, is  $e = 1.30$  so that the well in the nonmonotonic interacting potential is very small. In this case there is visible admixture of the current of second component in vortices inside the cluster, though its current is predominantly concentrated on the boundary of the cluster.

### C. Non-compact vortex clusters and non-pairwise interactions

Next we report the regime where the passive second band (i.e. with positive  $\alpha_2$ ) is coupled to the first band by extremely strong Josephson coupling  $\eta = 7.0$  (shown on Fig. 4). This coupling imposes a strong energy penalty both for disparities of the condensates variations and for the difference between phases of the condensates. Besides that in that regime there is a relatively strong non-pairwise interactions which diminish the energetic benefits of a triangle-like states compared to line-like vortex states.<sup>30</sup> We get a flat and complicated energy landscape and the outcome of the energy minimization strongly depends on initial configuration. Simulations whose outcome is compact clusters like Fig. 2 and Fig. 3 clearly ground states, since various initial guesses lead to similar final configurations. Simulating systems like in Fig. 4 is less straightforward. Numerical evolution in these systems is extremely slow because of the very complicated energy landscape. The final state strongly depends on the initial field configuration, indicating the configuration is not ground state but a bound state with a very slow evolution. Formation of highly disordered states and vortex chains due to short-range nature of the attractive potentials and many-body forces was a common outcome of the simulation in the similar type-1.5 regimes with strong Josephson coupling, in spite of negligible effects of ultra-fine numerical grid.

The Fig. 4 shows the typical non-universal outcome of the energy minimization in this case. Striking feature here is formation of vortex stripe-like configuration. Indeed it strongly contradicts the ground state expected from the



two-body forces in this system. Namely the axially symmetric two-body potentials with long range attraction and short-range repulsion (which we have in this case) do not allow stripe formation in the ground state configurations. Nonetheless such structures are physically entirely possible: first the exponentially decaying short-range forces result in very tiny forces which can drive evolution from a stripe to compact cluster configuration. Secondly there are repulsive multibody intervortex forces which compromise system's ability for form a compact configuration.<sup>30</sup> So in that regime vortex stripes and small lines can easily form because of non-pairwise intervortex interactions.

Note that even in this regime, the system exhibits self-induced gradients of the phase difference, in spite of the strong Josephson coupling.

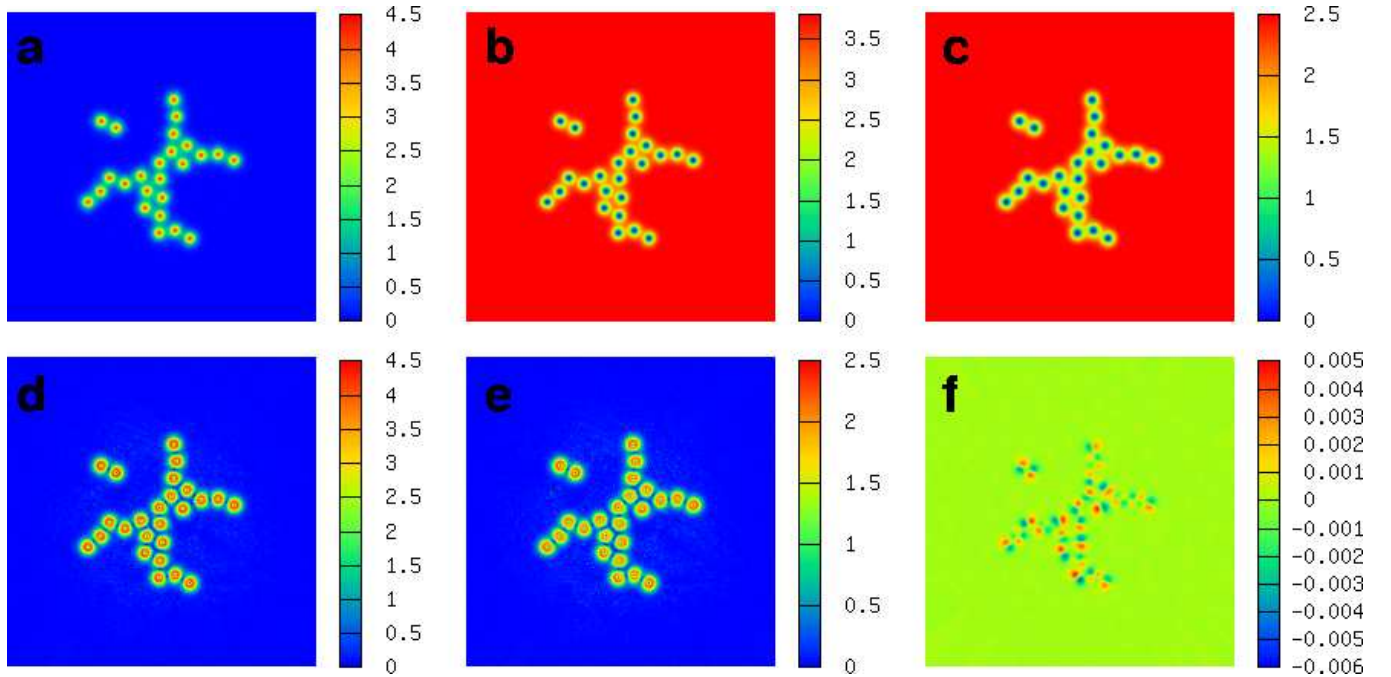


FIG. 4. A bound state of an  $N_v = 25$  vortex configuration in case when superconductivity in the second band is due to interband proximity effect and the Josephson coupling is very strong  $\eta = 7.0$ . The initial configuration in this simulation was a giant vortex. Other parameters are  $(\alpha_1, \beta_1) = (-1.00, 1.00)$ ,  $(\alpha_2, \beta_2) = (3.00, 0.50)$ ,  $e = 1.30$ . For the simulations, like the one shown on Fig. 3 the stopping criterion of energy minimization was when relative variation of the norm of the gradient of the GL functional with respect to all degrees of freedom to be less than  $10^{-6}$ . Here the situation is slightly different from that shown on two previous figures. Clearly in the shown above configuration the ground state was not reached. However the interaction potentials are such that the evolution at the later stages becomes extremely slow. The number of energy minimization steps in this case was order of magnitude larger than what was required for convergence in the previous regimes.

## V. SEMI-MEISSNER STATE AND BROKEN SYMMETRIES.

As discussed above a system with non-monotonic intervortex interaction potentials allow a state with macroscopic phase separation in vortex droplets and Meissner domains. In type-1.5 superconductors this state can also represent a phase separation into domains of states with different broken symmetries. In this section we will give two different examples of how such behavior can arise.

Note that in multicomponent superconductors some symmetries are global (i.e. associated with the degrees of freedom decoupled from vector potential) and some are local i.e. associated with the degrees of freedom coupled to vector potential. It is well known that in the later case the concept of spontaneous symmetry breakdown is not defined the same way as in a system with global symmetry. However below, for brevity we will not be making terminological distinctions between local and global symmetries (detailed discussion of these aspects can be found in e.g.<sup>20,23,43</sup>).

### A. Semi-Meissner state as a macroscopic phase separation in $U(1) \times U(1)$ and $U(1)$ domains.

Consider a superconductor with broken  $U(1) \times U(1)$  symmetry, i.e. a collection of independently conserved condensates with no intercomponent Josephson coupling. As discussed above, in the Semi-Meissner state in vortex droplets the superconducting component which has vortices with larger cores is more depleted. In  $U(1) \times U(1)$  system the vortices with phase windings in different condensates are bound electromagnetically which gives asymptotically logarithmic interaction potential with prefactor proportional to  $|\psi_1|^2|\psi_2|^2/(|\psi_1|^2 + |\psi_2|^2)$ ,<sup>43</sup> and even weaker interaction strength at shorter separations.

Consider now a macroscopically large vortex domain. Even if the second component there is not completely depleted, its density is suppressed and as a consequence the binding energy between vortices with different phase windings ( $\Delta\theta_1 = 2\pi, \Delta\theta_2 = 0$ ) and ( $\Delta\theta_1 = 0, \Delta\theta_2 = 2\pi$ ) can be arbitrarily small. Moreover the vortex ordering energy in the component with more depleted density will also small. As a result, even small thermal fluctuation can drive vortex sublattice melting transition<sup>20,22</sup> in the macroscopically large vortex droplet. In that case the fractional vortices in weaker component tear themselves off the fractional vortices in strong component and form a disordered state. Note that the vortex sublattice melting is associated with the phase transition from  $U(1) \times U(1)$  to  $U(1)$  state.<sup>20,22</sup> I.e. that vortex cluster will represent a domain of  $U(1)$  phase (associated with the superconducting state of strong component) immersed in domain of vortexless  $U(1) \times U(1)$  Meissner state. If the magnetic field is increased the system will go from the Semi-Meissner state (with coexisting  $U(1) \times U(1)$  and  $U(1)$  domains) to  $U(1)$  vortex state.

### B. Semi-Meissner state as a macroscopic phase separation in $U(1)$ and $U(1) \times Z_2$ domains in three band type-1.5 superconductors.

In the previous subsection we considered the case where Semi-Meissner state represents coexistences of domains with different broken symmetries as a consequence of vortex sublattice melting transition. In type-1.5 systems the coexistence of domains with different broken symmetry can also take place also in the ground state, i.e. without the need of thermal fluctuations.<sup>44</sup> In this subsection we discuss an example studied in Ref.<sup>44</sup> of such behavior in a three-band model with “phase frustration”.

The minimal GL free energy functional to model a three-band superconductor is

$$F = \frac{1}{2}(\nabla \times \mathbf{A})^2 + \sum_{i=1,2,3} \frac{1}{2} |\mathbf{D}\psi_i|^2 + \alpha_i |\psi_i|^2 + \frac{1}{2} \beta_i |\psi_i|^4 + \sum_{i=1,2,3} \sum_{j>i} \eta_{ij} |\psi_i| |\psi_j| \cos(\varphi_{ij}). \quad (22)$$

Here the phase difference between two condensates are denoted  $\varphi_{ij} = \varphi_j - \varphi_i$ .

Systems with more than two Josephson-coupled bands can exhibit *phase frustration*.<sup>35,44,45</sup> For  $\eta_{ij} < 0$ , a given Josephson interaction energy term is minimal for zero phase difference (we then refer to the coupling as “phase-locking”), while when  $\eta_{ij} > 0$  it is minimal for a phase difference equal to  $\pi$  (we then refer to the coupling as “phase-antilocking”). Two component systems are symmetric with respect to the sign change  $\eta_{ij} \rightarrow -\eta_{ij}$  as the phase difference changes by a factor  $\pi$ , for the system to recover the same interaction. However, in systems with more than two bands there is generally no such symmetry. For example if a three band system has  $\eta > 0$  for all Josephson interactions, then these terms can not be simultaneously minimized, as this would correspond to all possible phase differences being equal to  $\pi$ .

The ground state values of the fields  $|\psi_i|$  and  $\varphi_{ij}$  of system (22) are found by minimizing its potential energy

$$\sum_i \left\{ \alpha_i |\psi_i|^2 + \frac{1}{2} \beta_i |\psi_i|^4 \right\} + \sum_{j>i} \eta_{ij} |\psi_i| |\psi_j| \cos(\varphi_{ij}). \quad (23)$$

Minimizing the potential energy (23) can not in general be done analytically. Yet, some properties can be derived from qualitative arguments. In terms of the sign of the  $\eta$ 's, there are four principal situations:

Case	Sign of $\eta_{12}, \eta_{13}, \eta_{23}$	Ground State Phases
1	— — —	$\varphi_1 = \varphi_2 = \varphi_3$
2	— — +	Frustrated
3	— + +	$\varphi_1 = \varphi_2 = \varphi_3 + \pi$
4	+ + +	Frustrated

The case 2) can result in several ground states. If  $|\eta_{23}| \ll |\eta_{12}|, |\eta_{13}|$ , then the phase differences are generally  $\varphi_{ij} = 0$ . If on the other hand  $|\eta_{12}|, |\eta_{13}| \ll |\eta_{23}|$  then  $\varphi_{23} = \pi$  and  $\varphi_{12}$  is either 0 or  $\pi$ . For certain parameter values it can also have compromise states with  $\varphi_{ij}$  not being integer multiples of  $\pi$ .

The case 4) can give a wide range of ground states, as can be seen in Fig. 5. As  $\eta_{12}$  is scaled, ground state phases change from  $(-\pi, \pi, 0)$  to the limit where one band is depleted and the remaining phases are  $(-\pi/2, \pi/2)$ .

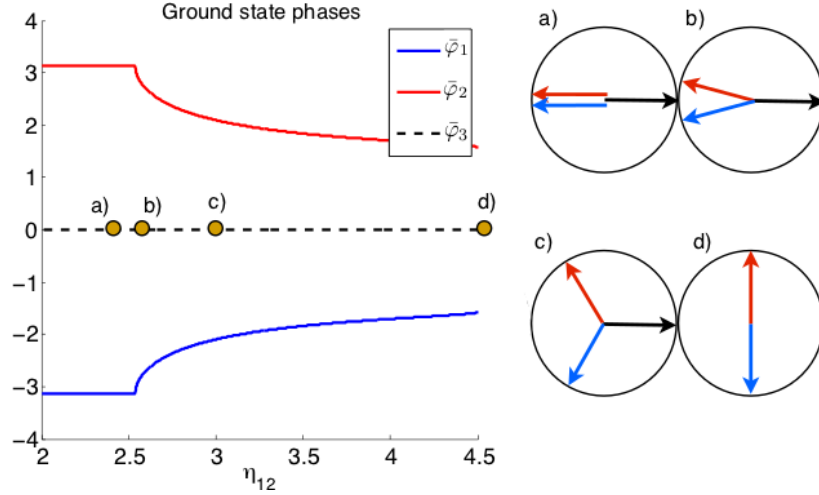


FIG. 5. Ground state phases of the three components as function of  $\eta_{12}$  (here  $\varphi_3 = 0$  fixes the gauge). The GL parameters are  $\alpha_i = 1$ ,  $\beta_i = 1$ ,  $\eta_{13} = \eta_{23} = 3$ . For intermediate values of  $\eta_{12}$  the ground state exhibits discrete degeneracy (symmetry is  $U(1) \times Z_2$  rather than  $U(1)$ ) since the energy is invariant under the sign change  $\varphi_2 \rightarrow -\varphi_2$ ,  $\varphi_3 \rightarrow -\varphi_3$ . For large  $\eta_{12}$  we get  $\varphi_2 - \varphi_3 = \pi$  implying that  $|\psi_3| = 0$  and so there is a second transition from  $U(1) \times Z_2$  to  $U(1)$  and only two bands at the point d). Here, the phases were computed in a system with only passive bands, though systems with active bands exhibit the same qualitative properties except for the transition to  $U(1)$  and two bands only (*i.e.* active bands have non-zero density in the ground state).

An important property of the potential energy (23) is that if any of the phase differences  $\varphi_{ij}$  is not an integer multiple of  $\pi$ , then the ground state possesses an additional discrete  $Z_2$  degeneracy. For example for a system with  $\alpha_i = -1$ ,  $\beta_i = 1$  and  $\eta_{ij} = 1$ , two possible ground states are given by  $\varphi_{12} = 2\pi/3$ ,  $\varphi_{13} = -2\pi/3$  or  $\varphi_{12} = -2\pi/3$ ,  $\varphi_{13} = 2\pi/3$ . Thus in this case, the symmetry is  $U(1) \times Z_2$ , as opposed to  $U(1)$ . As a result, like any other system with  $Z_2$  degeneracy, the theory allows an additional set of topological excitations : domain walls interpolating between the two inequivalent ground states.

The ground state of a phase frustrated superconductor is in many cases non-trivial, with phase differences being compromises between the various interaction terms. Inserting vortices in such a system can shift the balance between different competing couplings, since vortices can in general have different effects on the different bands. In particular, since the core sizes of vortices are not generally the same in all bands, vortex matter will typically deplete some components more than others and thus can alter the preferred values of the phase difference. So the minimal potential energy inside a vortex lattice or cluster may correspond to a different set of phase differences than in the vortexless ground state. To see this, consider the following argument: The phase-dependent potential terms in the free energy (22) are of the form

$$\eta_{ij} u_i u_j f_i(\mathbf{r}) f_j(\mathbf{r}) \cos(\varphi_{ij}(\mathbf{r})), \quad (24)$$

where  $u_i$  are ground state densities and each  $f_i(\mathbf{r})$  represent an Ansatz which models how superfluid densities are modulated due to vortices. Consider now a system where  $N$  vortices are uniformly distributed in a domain  $\Omega$ . The phase dependent part of the free energy is

$$U_\varphi = \left[ \sum_{i>j} \eta_{ij} u_i u_j \right] \int_\Omega d\mathbf{r} f_i(\mathbf{r}) f_j(\mathbf{r}) \cos(\varphi_{ij}(\mathbf{r})). \quad (25)$$

If  $\varphi_{ij}$  is varying slowly in comparison with the inter vortex distance, then it can be considered constant in a uniform distribution of vortices (as a first approximation). In that case (25) can be approximated by

$$U_\varphi \simeq \sum_{ij} \tilde{\eta}_{ij} u_i u_j \cos(\varphi_{ij}) \text{ where } \tilde{\eta}_{ij} = \eta_{ij} \int_\Omega d\mathbf{r} f_i(\mathbf{r}) f_j(\mathbf{r}) \quad (26)$$

If on the other hand  $\varphi_{ij}$  varies rapidly, then it is not possible to define  $\tilde{\eta}_{ij}$  without a spatial dependence. Then  $\varphi_{ij}$  will depend on  $\tilde{\eta}_{ij}(\mathbf{r})$  which is related to the local modulation functions  $f_i f_j$  and vary with a characteristic length scale.

Thus,  $\tilde{\eta}$  is the effective inter-band interaction coupling resulting from density modulation. Since in general,  $f_i \neq f_j$  (unless the two bands  $i, j$  are identical), one must take into account the modulation functions  $f_i$  when calculating the phase differences. In particular, if the core size in component  $i$  is larger than in component  $j$ , then  $\int d\mathbf{r} f_i f_k < \int d\mathbf{r} f_j f_k$  and therefore the phase differences  $\varphi_{ij}$  minimizing (26) depend on  $f_i$ , and consequently on the density of vortices. Roughly speaking, introducing vortices in the system is equivalent to relative effective decrease of some of the Josephson coupling constants.

This can have profound consequences, as the symmetry of the problem depends on the Josephson interaction terms. In Figs. 6, 7 we see a type-1.5 system in which the symmetry of the ground state is  $U(1)$ . As vortices are inserted into the system, they form clusters and the effective inter band interactions  $\tilde{\eta}_{ij}$  are renormalized to a degree that the symmetry of the domain near vortex clusters changes to  $U(1) \times Z_2$ . Thus the Semi-Meissner state in such a system represents macroscopic phase separation in domains of broken  $U(1)$  and  $U(1) \times Z_2$  symmetries.

## VI. MICROSCOPIC THEORY OF TYPE-1.5 SUPERCONDUCTIVITY

The phenomenological Ginzburg-Landau model described above predict the possibility of 1.5 superconducting state. Formally the GL theory applies only at elevated temperatures. To describe type-1.5 superconductivity in all temperature regimes (except, indeed the region where mean-field theory is inapplicable) as well as to make a connection with a certain class of the real systems requires a microscopic approach which also does not rely on a GL expansion. Such a theory was recently developed in.<sup>28</sup> So let us consider the described above physics in a microscopic formalism of self-consistent Eilenberger theory. We consider a superconductor with two overlapping bands at the Fermi level.<sup>9</sup> The corresponding two sheets of the Fermi surface are assumed to be cylindrical. Within quasi-classical approximation the band parameters characterizing the two different sheets of the Fermi surface are the Fermi velocities  $V_{Fj}$  and the partial densities of states (DOS)  $\nu_j$ , labeled by the band index  $j = 1, 2$ . We normalize the energies to the critical temperature  $T_c$  and length to  $r_0 = \hbar V_{F1}/T_c$ . The system of Eilenberger equations for two bands is

$$\begin{aligned} v_{Fj} \mathbf{n}_p (\nabla + i\mathbf{A}) f_j + 2\omega_n f_j - 2\Delta_j g_j &= 0, \\ v_{Fj} \mathbf{n}_p (\nabla - i\mathbf{A}) f_j^+ - 2\omega_n f_j^+ + 2\Delta_j^* g_j &= 0. \end{aligned} \quad (27)$$

Here  $\omega_n = (2n+1)\pi T$  are Matsubara frequencies and  $v_{Fj} = V_{Fj}/V_{F1}$ . The vector  $\mathbf{n}_p = (\cos \theta_p, \sin \theta_p)$  parameterizes the position on 2D cylindrical Fermi surfaces. The quasi-classical Green's functions in each band obey normalization condition  $g_j^2 + f_j f_j^+ = 1$ . The Eilenberger differential Eqs.(27) are solved together with the integral self-consistency equations for the gaps

$$\Delta_i = T \sum_{n=0}^{N_d} \int_0^{2\pi} \lambda_{ij} f_j d\theta_p \quad (28)$$

$$\mathbf{j} = -\frac{T}{\kappa^2} \sum_{j=1,2} n_j v_{Fj} \sum_{n=0}^{N_d} \text{Im} \int_0^{2\pi} \mathbf{n}_p g_j d\theta_p. \quad (29)$$

Here  $\lambda_{ij}$  is the coupling matrix which satisfies the symmetry relations  $n_1 \lambda_{12} = n_2 \lambda_{21}$  where  $n_i$  are the partial DOS normalized so that  $n_1 + n_2 = 1$ . We consider  $\lambda_{11} > \lambda_{22}$  and therefore refer to the first band as “strong” and to the second as “weak”.

The asymptotics of the gap functions  $|\Delta_{1,2}|(r)$  at distances far from the vortex core can be found linearizing the Eilenberger Eqs.(27) together with the self-consistency equations. The asymptotics of the linearized system is governed by the singularities of response function found in Ref.(<sup>28</sup>) among which are the poles and branch cuts. In general there are two regimes regulating the asymptotic behavior of gap functions. The first regime is realized when two poles of the response function lie below the branch cut. The two poles determine the *two inverse length scales* or, equivalently, the two masses of composite gap functions fields (i.e. linear combinations of the fields as in the previous section), which we denote as “heavy”  $\mu_H$  and “light”  $\mu_L$  (i.e.  $\mu_H > \mu_L$ ). At elevated temperatures these masses are exactly the same as the given by a corresponding two-component GL theory obtained by the gradient expansion from the microscopic theory.<sup>29</sup> The GL theory can be also used to describe the two massive modes at relatively low temperatures.<sup>29</sup> In this case the coefficients should be adjusted phenomenologically in order to obtain the same values of masses as the microscopic theory yields.

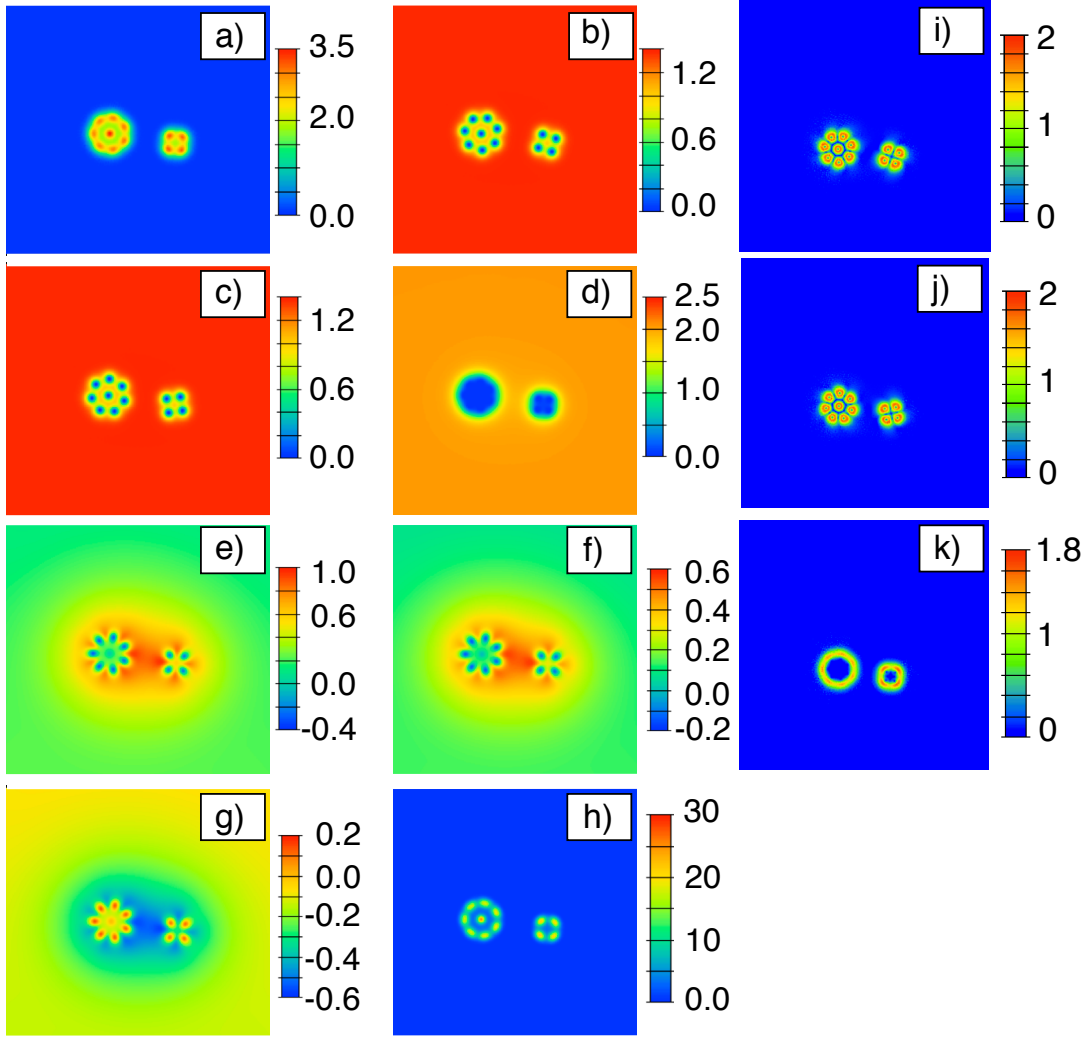


FIG. 6. Interacting vortex clusters with internal  $Z_2$  symmetry in a frustrated three band superconductor. The snapshot represents a non-stationary state of the weakly interacting well-separated clusters. In this numerical computation, each of the clusters has with a good accuracy converged to a physical solution of GL equations, but the snapshot is taken during the slow evolution driven by the weak intercluster interaction. The snapshot demonstrates the existence of long-range field variations associated with the soft mode. This produces long-range weak intervortex forces. Displayed quantities are: a) Magnetic field, b-d)  $|\psi_1|^2, |\psi_2|^2, |\psi_3|^2$ , e)  $|\psi_1||\psi_2|\sin\varphi_{12}$ , f)  $|\psi_1||\psi_3|\sin\varphi_{13}$ , g)  $|\psi_1||\psi_3|\sin\varphi_{23}$ . The GL parameters are  $\alpha_1 = -3$ ,  $\beta_1 = 3$ ,  $\alpha_2 = -3$ ,  $\beta_2 = 3$ ,  $\alpha_3 = 2$ ,  $\beta_3 = 0.5$ ,  $\eta_{12} = 2.25$ ,  $\eta_{13} = -3.7$ . The parameter set was chosen so that it lies in the regime where the ground state symmetry of the system without vortices is  $U(1)$ , but is close to the  $U(1) \times Z_2$  region. Because of the disparity in vortex core size the effective interaction strengths  $\tilde{\eta}_{ij}$  are depleted to different extents. As a consequence, the symmetry associated with the effective couplings inside the cluster correspond to the  $U(1) \times Z_2$  regime.

The second regime is realized at lower temperatures when there is only one pole below the branch cut, In this case the asymptotic is determined by the light mass mode  $\mu_L$  and the contribution of the branch cut which has all the length scales smaller than some threshold one determined by the position of the lowest branch cut on the imaginary axis. The branch cut contribution is essentially non-local effect which is not captured by GL theory therefore one can expect growing discrepancies between effective GL solution and the result of microscopic theory at low temperatures.

The examples from ref.<sup>28</sup> of the temperature dependencies of the masses  $\mu_{L,H}(T)$  are shown in the Fig.8. The evolution of the masses  $\mu_{L,H}$  is shown in the sequence of plots Fig.8(a)-(d) for  $\lambda_J$  increasing from the small values  $\lambda_J \ll \lambda_{11}, \lambda_{22}$  to the values comparable to intraband coupling  $\lambda_J \sim \lambda_{11}, \lambda_{22}$ . The two massive modes coexist at the temperature interval  $T_1^* < T < T_c$ , where the temperature  $T_1^*$  is determined by the branch cut position, shown in the Fig.8 by black dashed line. For temperatures  $T < T_1^*$  there exists only one massive mode lying below the branch cut. At very low temperatures the mass  $\mu_L$  is very close to the branch cut. As the interband coupling parameter is



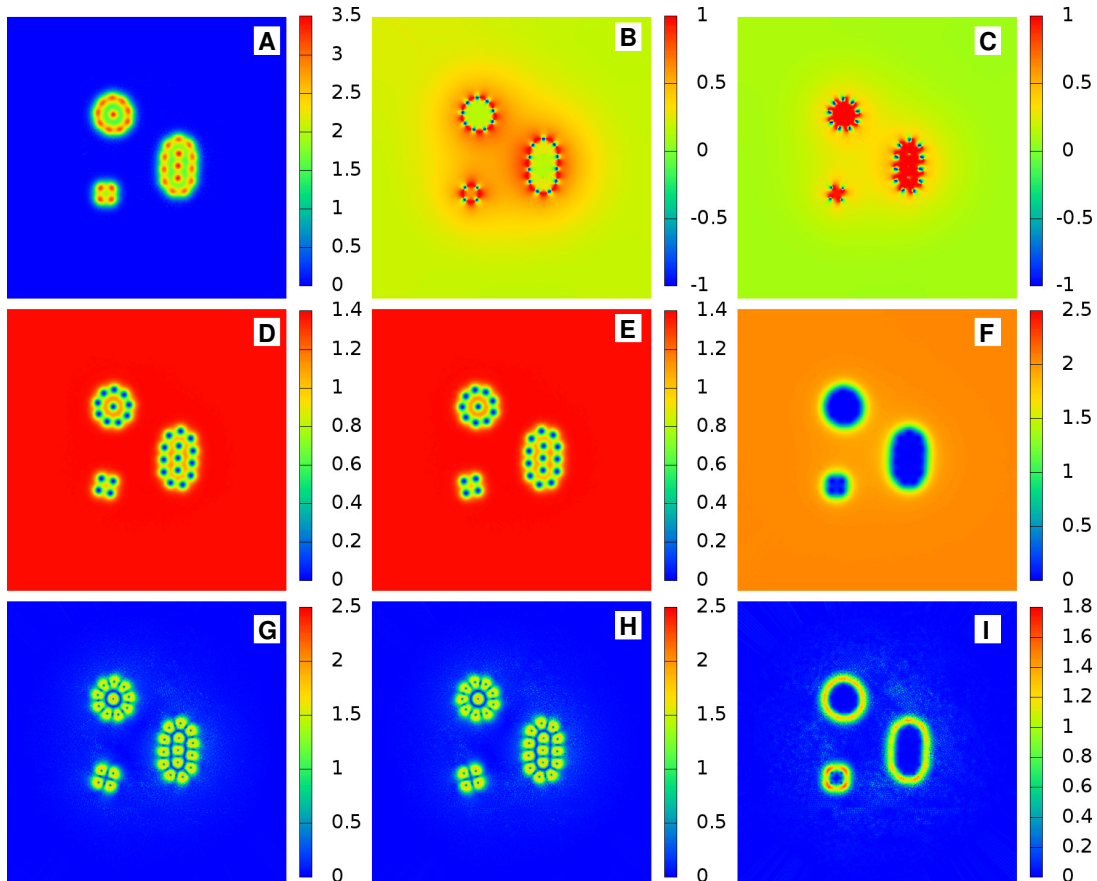


FIG. 7. Interacting vortex clusters with internal  $Z_2$  symmetry in a frustrated three band superconductor. The panel **A** displays the magnetic field  $B$ . Panels **B** and **C** respectively display  $\sin \varphi_{12}$  and  $\sin \varphi_{13}$ , the third phase difference can obviously be obtained from these two ones. Second line, shows the densities of the different condensates  $|\psi_1|^2$  (**D**),  $|\psi_2|^2$  (**E**),  $|\psi_3|^2$  (**F**). The third line displays the supercurrent densities associated with each condensate  $|J_1|$  (**G**),  $|J_2|$  (**H**),  $|J_3|$  (**I**). The parameter set here is the same as in Fig. 6. The instructive difference here is that the sine of the phase differences is represented ‘unweighted’ by the densities in contrast to Fig. 6. Panel **C** now makes clear that the inner cluster is in a defined state  $\varphi_{13} \approx \pi/2$  (whose opposite state would have been  $-\pi/2$ ). Panel **B** gives a visualization of the long range interaction between the clusters.

increased, the temperature  $T_1^*$  rises and becomes equal to  $T_c$  at some critical value of  $\lambda_J = \lambda_{Jc}$ .

Besides justifying the predictions of phenomenological two-component GL theory<sup>29</sup> the microscopic formalism developed in Ref.(<sup>28</sup>) allows to describe type-1.5 superconductivity beyond the validity of GL models. The type-1.5 behavior requires a density mode with low mass  $\mu_L$  to mediate intervortex attraction at large separations, which should coexist with short-range repulsion. In ref.<sup>28</sup> find that the temperature dependence of  $\mu_L(T)$  is characterized by an anomalous behavior, which is in strong contrast to temperature dependence of the mass of the gap mode in single-band theories. As shown on Fig.9a the function  $\mu_L(T)$  is *non-monotonic* at low temperatures.

Therefore for a certain range of parameters in contrast with the physics of single-band superconductors the product of London penetration depth  $\Lambda$  and  $\mu_L$  has a strong and nonmonotonic temperature dependence shown in Fig.9b. The inverse of the mass of the light composite gap mode  $\mu_L$  sets the range of the attractive density-density contribution to intervortex interaction. Therefore the condition for the occurrence of the intervortex attraction will be met if  $\Lambda\mu_L < 1$ . Note that only *infinitesimally* close to  $T_c$ , the product can be interpreted as single-component-like GL parameter  $\kappa$  because the inverse mass  $\sqrt{2\mu_L^{-1}}$  becomes the GL coherence length. However as shown on Fig. 9 b) this GL parameter can have a very strong temperature dependence, thus in general it *cannot* be used as a single parameter to characterize two-band systems. This is because in a two-band superconductor, for a wide range of parameters even slightly away from  $T_c$  the temperature dependence of  $\mu_L$ , is dramatically different from that of the inverse magnetic field penetration length  $\Lambda^{-1}$ .

Furthermore because the softest mode with the mass  $\mu_L$  in two band system may be associated with only a fraction of the total condensate (as follows from corresponding mixing angles), and because there could be the second mixed gap mode with larger mass  $\mu_H$ , the short-range intervortex interaction can be repulsive. In Ref.(<sup>28</sup>) the temperature



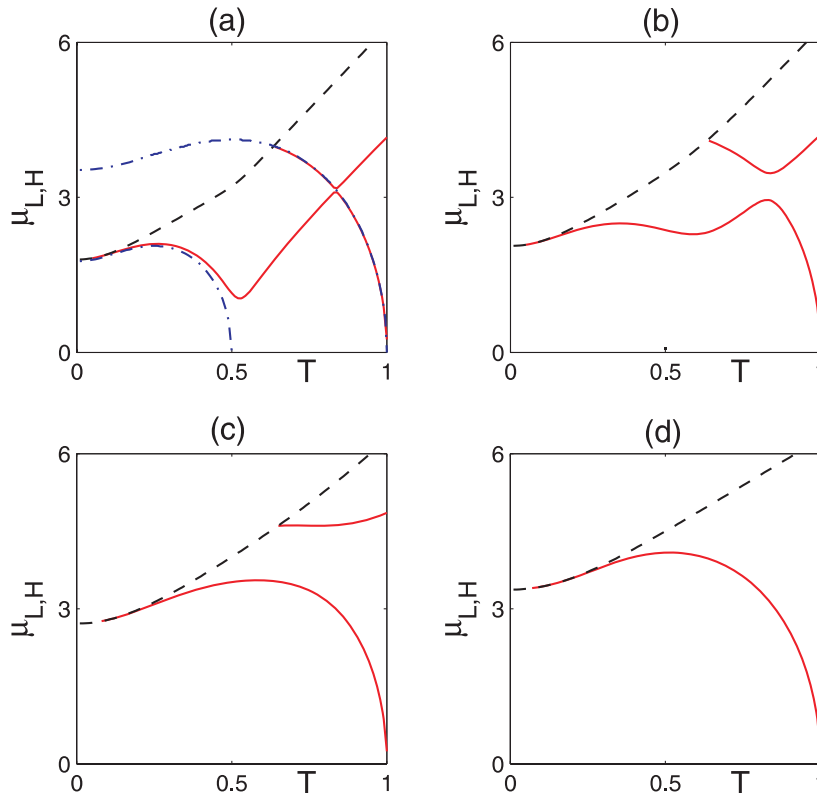


FIG. 8. Calculated in<sup>28</sup> masses  $\mu_L$  and  $\mu_H$  (red solid lines) of the composite gap function fields for the different values of interband Josephson coupling  $\lambda_J$  and  $\gamma_F = 1$ . In the sequence of plots (a)-(d) the transformation of masses is shown for  $\lambda_J$  decreasing from the small values  $\lambda_J \ll \lambda_{11}, \lambda_{22}$  to the values comparable to intraband coupling  $\lambda_J \sim \lambda_{11}, \lambda_{22}$ . The particular values of coupling constants are  $\lambda_{11} = 0.25$ ,  $\lambda_{22} = 0.213$  and  $\lambda_J = 0.0005$ ;  $0.0025$ ;  $0.025$ ;  $\lambda_{22}$  for plots (a-d) correspondingly. By black dash-dotted lines the branch cuts are shown. In (a) with blue dash-dotted lines the masses of modes are shown for the case of  $\lambda_J = 0$ . Note that at  $\lambda_J = 0$  the two masses go to zero at two different temperatures. Because  $1/\mu_{L,H}$  are related to the coherence length, this reflects the fact that for  $U(1) \times U(1)$  theory there are two independently diverging coherence lengths. Note that for finite values of interband coupling only one mass  $\mu_L$  goes to zero at one  $T_c$ : this is in turn a consequence of the fact that Josephson coupling breaks the symmetry down to single  $U(1)$ .

dependencies of  $\Lambda^{-1}$  and  $\mu_L$  are compared demonstrating how in these cases the system goes from type-II to type-1.5 behavior as temperature is decreased and  $\mu_L$  becomes smaller than  $\Lambda^{-1}$ , and, the density associated with the light mode is small enough that the system has a short-range intervortex repulsion.

We calculate self-consistently the structure of isolated vortex for different values of  $\gamma_F = v_{F2}/v_{F1}$ . A complex aspect of the vortex structure in two-band system is that in general the exponential law of the asymptotic behavior of the gaps is *not* directly related to the “core size” at which gaps recover most of their ground state values. We can characterize this effect by defining a “healing” length  $L_{\Delta i}$  of the gap function as follows  $|\Delta_i|(L_{\Delta i}) = 0.95\Delta_{i0}$ . The characteristic example of the vortex structure is shown in Fig. 9(c). For this case we obtain that  $L_{\Delta 1} \approx 0.8$  for all values of  $\gamma_F$ . On the contrary, the healing length  $L_{\Delta 2}$  of changes significantly such that  $L_{\Delta 2} = 1.6$ ;  $2.5$ ;  $3.2$ ;  $3.9$ ;  $4.5$  for  $\gamma_F = 1$ ;  $2$ ;  $3$ ;  $4$ ;  $5$  correspondingly.

To demonstrate the type-1.5 superconductivity i.e. large-scale attraction and small-scale repulsion of vortices which originates from disparity of the variations of two gaps, the intervortex interaction energy was calculated in<sup>28</sup>. The two-band generalization of the Eilenberger expression was evaluated for the free energy of the two vortices positioned at the points  $\mathbf{r}_R = (d/2, 0)$  and  $\mathbf{r}_L = (-d/2, 0)$  in  $xy$  plane. In Fig.9(d) the interaction energy  $E_{int}$  is shown as a function of the distance between two vortices  $d$ . The energy  $E_{int}$  is normalized to the single vortex energy  $E_v$ . The plots on Fig.9(d) clearly demonstrate the emergence of type-1.5 behavior when the parameter  $\gamma_F$ , which characterizes the disparity in band characteristics is increased. This is manifested in the appearance non-monotonic behavior of the intervortex interaction energy  $E_{int}(d)$  as a consequence of two-component structure of the theory.

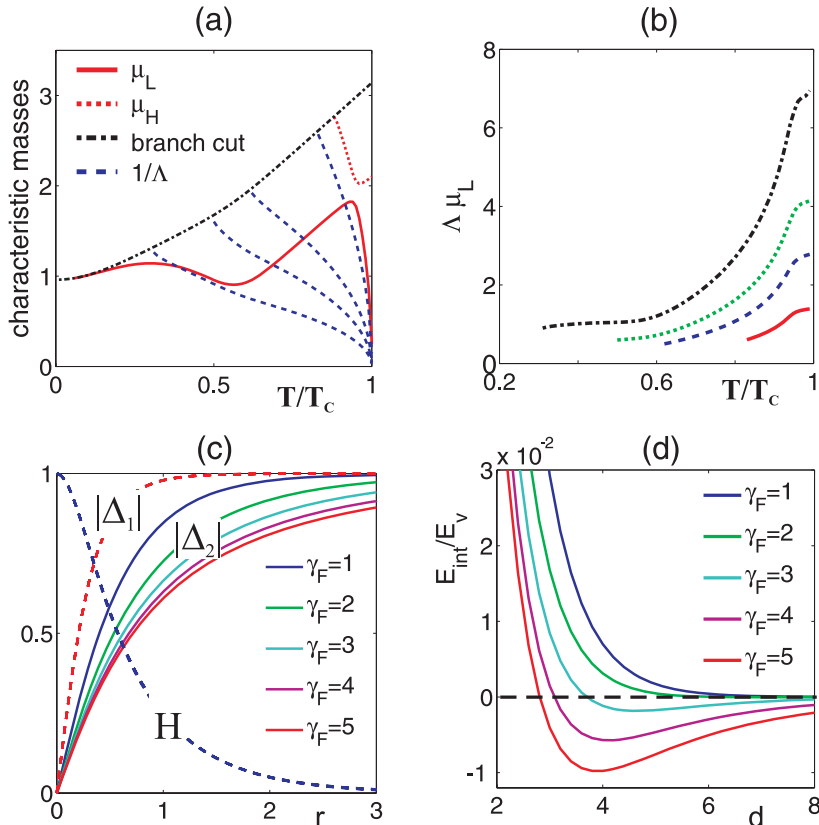


FIG. 9. Calculated in ref.<sup>28</sup> (a) Masses  $\mu_L$  and  $\mu_H$  (red solid and dotted lines) of the composite gap function fields and inverse London penetration (blue dashed lines) for the different values of  $\Lambda\mu_L(T_c)/\sqrt{2} = 1; 2; 3; 5$ . The position of branch cut is shown by black dash-dotted line. (b) The temperature dependence of the quantity  $\Lambda\mu_L$  for  $\Lambda\mu_L(T_c)/\sqrt{2} = 1; 2; 3; 5$  (red solid, blue dashed and black dash-dotted lines). (c) Distributions of magnetic field  $H(r)/H(r=0)$ , gap functions  $|\Delta_1|(r)/\Delta_{10}$  (dashed lines) and  $|\Delta_2|(r)/\Delta_{20}$  (solid lines) for the coupling parameters  $\lambda_{11} = 0.25$ ,  $\lambda_{22} = 0.213$  and  $\lambda_{21} = 0.0025$  and different values of the band parameter  $\gamma_F = 1; 2; 3; 4; 5$ . (d) The energy of interaction between two vortices normalized to the single vortex energy as function of the intervortex distance  $d$ . In panels (c,d) the temperature is  $T = 0.6$ .

## VII. CONCLUSION

We reviewed the recent developments in description of type-1.5 superconductivity in multicomponent systems. Both at the levels of microscopic and Ginzburg-Landau field theories the behavior arises as a consequence of one or several of the fundamental length scales associated with density variations  $\xi_i$  being larger than the magnetic field penetration length  $\lambda$ , while at the same time the system possessing thermodynamically stable vortex excitations. These vortices have long-range attractive (originating from outer cores overlap) and short-range repulsive interaction. This leads to an additional “semi-Meissner” phase sandwiched between Meissner and vortex states which is a macroscopic phase separation into domains of Meissner and vortex states. We discussed that in case of thermal fluctuations or/and more that two bands this phase separation can also result in coexistence of macroscopically large domains with different broken symmetries: i.e.  $U(1)$  and  $U(1) \times U(1)$  or  $U(1)$  and  $U(1) \times Z_2$ .

## VIII. ACKNOWLEDGMENTS

EB was supported by Knut and Alice Wallenberg Foundation through the Royal Swedish Academy of Sciences, Swedish Research Council and by the US National Science Foundation CAREER Award No. DMR-0955902. JC was supported by the Swedish Research Council. MS was supported by the Swedish Research Council, “Dynasty” foundation, Presidential RSS Council (Grant No. MK-4211.2011.2) and Russian Foundation for Basic Research. JMS was supported by the UK Engineering and Physical Sciences Research Council. EB thanks the Aspen Center for Physics for hospitality and support under the NSF grant No. 1066293. The computations were performed on

resources provided by the Swedish National Infrastructure for Computing (SNIC) at National Supercomputer Center at Linköping, Sweden.

- 
- <sup>1</sup> V.L. Ginzburg and L.D. Landau, Zh. Eksp. Teor. Fiz. 20, 1064 (1950)
  - <sup>2</sup> P.G. de Gennes, *Superconductivity of metals and alloys* (New York: Addison-Wesley, 1989).
  - <sup>3</sup> L. Landau, Nature (London, United Kingdom) **141**, 688 (1938). R. P. Huebener, *Magnetic Flux Structures of Superconductors*, 2nd ed. (Springer-Verlag, New-York, 2001). R. Prozorov, A. F. Fidler, J. Hoberg, P. C. Canfield, Nature Physics **4**, 327 - 332 (2008)
  - <sup>4</sup> A. Abrikosov Sov. Phys. JETP **5**, 1174 (1957)
  - <sup>5</sup> L. Kramer Phys. Rev. B **3**, 38213825 (1971);
  - <sup>6</sup> E. B. Bogomolny, Sov. J. Nucl. Phys. **24**, 449 (1976) [Yad. Fiz. **24**, 861 (1976)].
  - <sup>7</sup> A.E. Jacobs, Journal of Low Temp. Phys., **10**, 137 (1973).
  - <sup>8</sup> Johan Carlstrom, Egor Babaev, Martin Speight Phys. Rev. B **83**:174509,2011
  - <sup>9</sup> H. Suhl, B. T. Matthias, and L. R. Walker Phys. Rev. Lett. **3**, 552 (1959)
  - <sup>10</sup> A. Liu, I.I. Mazin, J. Kortus, Phys. Rev. Lett. **87** 087005 (2001); I.I. Mazin, et al., Phys. Rev. Lett. **89** (2002) 107002.
  - <sup>11</sup> X. X. Xi Rep. Prog. Phys. **71** 116501 (2008)
  - <sup>12</sup> A. Gurevich, Phys. Rev. B **67** 184515 (2003) ;
  - <sup>13</sup> A. Gurevich, Physica C **056** 160 (2007)
  - <sup>14</sup> M. E. Zhitomirsky and V.-H. Dao, Phys. Rev. B **69**, 054508 (2004).
  - <sup>15</sup> A. E. Koshelev, A. A. Golubov Phys. Rev. Lett., **92**, 107008 (2004)
  - <sup>16</sup> K. Tanaka, M. Eschrig, D.F. Agterberg, Phys. Rev. B **75**, 214512 (2007). K. Tanaka, D.F. Agterberg, J. Kopu, M. Eschrig Phys. Rev. B **73**, 220501(R) (2006)
  - <sup>17</sup> see e.g. K. Ishida, Y. Nakai, H. Hosono, J. Phys. Soc. Jpn. **78** 062001 (2009);
  - <sup>18</sup> L. J. Li , T. Nishio , Z. A. Xu , and V. V. Moshchalkov Phys. Rev. B **83**, 224522 (2011)
  - <sup>19</sup> N.W. Ashcroft, J. Phys. Condens. Matter **12**, A129 (2000); Phys. Rev. Lett. **92**, 187002 (2004)
  - <sup>20</sup> E. Babaev, A. Sudbø and N.W. Ashcroft Nature **431** 666 (2004),
  - <sup>21</sup> E. Babaev, N.W. Ashcroft Nature Physics **3**, 530 (2007)
  - <sup>22</sup> E. Smørgrav, J. Smiseth, E. Babaev, A. Sudbø Phys. Rev. Lett. **94**, 096401 (2005)
  - <sup>23</sup> E. V. Herland, E. Babaev, A. Sudbø Phys. Rev. B **82**, 134511 (2010)
  - <sup>24</sup> P. B. Jones, Mon. Not. Royal Astr. Soc. **371**, 1327 (2006); E. Babaev, Phys. Rev. Lett. **103**, 231101 (2009).
  - <sup>25</sup> E. Babaev & J.M. Speight Phys. Rev. B **72** 180502 (2005)
  - <sup>26</sup> E. Babaev, J. Carlstrom, J. M. Speight Phys. Rev. Lett. **105**, 067003 (2010)
  - <sup>27</sup> V.V. Moshchalkov, M Menghini, T. Nishio, Q. H. Chen, A. V. Silhanek, V. H. Dao, L. F. Chibotaru, N. D. Zhigadlo, and J. Karpinski Phys. Rev. Lett. **102**, 117001 (2009)
  - <sup>28</sup> M. Silaev and E. Babaev Phys. Rev. B **84**, 094515 (2011)
  - <sup>29</sup> M. Silaev and E. Babaev arXiv:1110.1593
  - <sup>30</sup> Johan Carlstrom, Julien Garaud, Egor Babaev Phys. Rev. B **84**, 134515 (2011)
  - <sup>31</sup> T. Nishio, Q. Chen, W. Gillijns, K. De Keyser, K. Vervaeke, and V. V. Moshchalkov Phys. Rev. B **81**, 020506(R) (2010); J. Gutierrez, B. Raes , A. V. Silhanek, L. J. Li, N. D. Zhigadlo, J. Karpinski, J. Tempere, and V. V. Moshchalkov Phys. Rev. B **85**, 094511 (2012)
  - <sup>32</sup> R. Geurts, M. V. Milosevic, F. M. Peeters Phys. Rev. B **81**, 214514 (2010)
  - <sup>33</sup> V. H. Dao, L. F. Chibotaru, T. Nishio, V. V. Moshchalkov Phys. Rev. B **83** 020503 (2011)
  - <sup>34</sup> Jun-Ping Wang, Physical Review B, **82**, 132505 (2010) Shi-Zeng Lin, Xiao Hu Phys. Rev. B **84**, 214505 (2011) C.J. Olson Reichhardt, C. Reichhardt, A.R. Bishop Phys. Rev. E **83**, 041501 (2011)
  - <sup>35</sup> Xiao Hu, Zhi Wang Phys. Rev. B **85**, 064516 (2012)
  - <sup>36</sup> S. A. Parameswaran, S. A. Kivelson, E. H. Rezayi, S. H. Simon, S. L. Sondhi, B. Z. Spivak arXiv:1108.0689
  - <sup>37</sup> A. A. Shanenko, M. V. Milosevic, F. M. Peeters, and A. V. Vagov. Phys. Rev. Lett. **106**, 047005 (2011); L. Komendova, M. V. Milosevic, A. A. Shanenko, F. M. Peeters Phys. Rev. B **84**, 064522 (2011) . These works propose a to use fourth-order in derivatives GL expansion. These works do not analyze asymptotics of a fourth order partial differential equations but use a numerical analysis of the “healing lengths” defined in a similar way as in.<sup>28</sup> In the first of this papers the healing lengths are called coherence length. It should however be noted that the healing lengths scales defined this way should not be confused with the coherence lengths discussed in the current paper since the healing lengths are largely determined by nonlinearities and are not associated with exponential fields asymptotics. In particular their behavior in the limit  $T \rightarrow T_c$  is principally different from that of coherence lengths calculated in.<sup>8,26,28,29</sup> One key aspect of the  $\tau$ -based GL expansion in this paper requires a correction. In these papers the leading order of the expansion yield field equations corresponding to a system with  $U(1) \times U(1)$  broken symmetry. The correct leading order GL expansion in two-band superconductors should however respect the broken  $U(1)$  symmetry of two-band superconductors.<sup>29</sup> Also, as discussed in<sup>29</sup> the GL functionals similar to those used in the current MS are justified on formal grounds (in a certain range of parameters) contrary what was stated in the above works.
  - <sup>38</sup> J.M. Speight, Phys. Rev. D **55** 3830 (1997) .

- <sup>39</sup> N.S. Manton and P.M. Sutcliffe, *Topological Solitons* (Cambridge University Press, Cambridge UK, 2004).
- <sup>40</sup> Nonpairwise interaction forces should arise in superconducting models beyond London approximation, when non-linearities become important. Long-range intervortex forces are described by a linear theory and thus are pairwise. In single-component GL model the nonlinear effects on interaction of three closely placed vortices were studied in A.Chaves, F. M. Peeters, G. A. Farias, and M. V. Milosevic Phys. Rev. B 83, 054516 (2011). Compared to single-component case, in two-component systems the non-pairwise forces are naturally different and much more diverse<sup>30</sup> because of the composite structure of vortex and thus more diverse ways a vortex can be deformed by its neighbors. Besides in contrast to single-component case, that they have direct influence on structure formation.
- <sup>41</sup> F. Hecht, O. Pironneau, A. Le Hyaric, K. Ohtsuka, Freefem++ (manual), 2007. <http://www.freefem.org>
- <sup>42</sup> <http://people.umass.edu/garaud/NonPairwise.html>. <http://www.youtube.com/user/QuantumVortices>.
- <sup>43</sup> E. Babaev Phys.Rev.Lett. **89** (2002) 06700; E. Babaev Nucl. Phys. B 686 **397** (2004); E. Babaev, J. Jaykka, and M. Speight, Phys. Rev. Lett. **103**, 237002 (2009); M.A. Silaev Phys. Rev. B 83, 144519 (2011)
- <sup>44</sup> Johan Carlstrom, Julien Garaud, Egor Babaev arXiv:1107.4279; Phys. Rev. B 84, 134518 (2011)
- <sup>45</sup> T. K. Ng and N. Nagaosa, Europhys. Lett. 87, 17003 (2009); V. Stanev and Z. Tesanovic, Phys. Rev. B 81, 134522 (2010); Y. Tanaka and T. Yanagisawa, Solid State Communications 150, 1980 (2010); Shi-Zeng Lin, Xiao Hu arXiv:1107.0814; Julien Garaud, Johan Carlstrom, Egor Babaev Phys. Rev. Lett. 107, 197001 (2011); V. Stanev arXiv:1108.2501